Effect of Film Thickness on F-doped TiO₂ Films Synthesized by Spin Coating Technique

Sweta

Department of Physics, Gurukula Kangri University, Haridwar, India. Corresponding author: shwetasharmaphy@gmail.com

Jeevitesh K. Rajput

Department of Physics, SRM Institute of Science and Technology, Delhi-NCR Campus, Modinagar, Ghaziabad, India. E-mail: Jeevitesh.phys@gmail.com

(Received on September 29, 2024; Revised on December 2, 2024 & December 12, 2024: Accepted on December 21, 2024)

Abstract

Fluorine-doped titanium dioxide (TiO₂) thin films were synthesised using a spin coating technique from titanium tetra isopropoxide, acetic acid, and ethanol. These films are coated on glass substrate for various coating cycles ranging from 5 to 30 and were further annealed at 450°C. For initial cycles, films are amorphous in nature. Films attains crystallization after coating cycle of 15. Films shows significant changes in the surface morphology, which depends on the coating cycle. Film thickness shows linear variation with coating cycle. Increase thickness result in the enhancement of crystallite size and relaxation of film as evidenced from peakwidth of X-ray diffraction patterns.

Keywords- Crystallite size, TiO₂, Fluorine doping, Spin-coating.

1. Introduction

Because of its extremely intriguing optical qualities, including its, high transmittance, high dielectric constant, high refractive index, and nontoxicity, titanium dioxide (TiO₂) is the metal oxide semi-conducting substance that has been the subject of most research (Ayorinde and Sayes, 2023; Marcelis et al., 2024). With all of these characteristics, it is a good candidate for a variety of technical uses, including wastewater treatment, glass defogging, self-cleaning, photo-catalysis, and antimicrobial sterilization (Fujishima et al., 2000).

TiO₂ is widely employed for the photodegradation of organic and inorganic contaminants due to environmental concerns, photovoltaic energy generation, and water photo splitting to produce hydrogen, optical filters (De et al., 2024), gas sensors (Zhao et al., 2024), wave-guides, DSSCs, PSCs, photocatalysts, and ceramic membranes (David et al., 2024).

The structural, and optical properties of TiO₂ are varied with different doping elements (Dubey et al., 2021). It is also reported that fluorine is a suitable candidate to enhance different properties of TiO₂ likewise surface morphology, crystalline phase and electronic structure (Subalakshmi and Senthilselvan, 2018). Fluorine doping is capable to modify the electronic structure by introducing new energy states, this impact also on electrical properties (Todorova et al., 2008). Chemical impurities, chemical precursors, and the synthesis process all have a significant impact on the concentration of these defects. As a matter of fact, temperature and pressure during the synthesis process are critical in regulating defect type and density. Amazing synthesis techniques, including chemical vapor deposition, wet chemistry, and physical approaches, were



employed for this goal (Choudhury and Choudhury, 2013). Important factors influencing the photo-electrocatalytic (PEC) performance, such as surface structure and lattice disorder, such as oxygen vacancies, are clarified by the work of Eftekhari et al. (2017). Thus, number of methods are utilized to synthesize TiO₂ nanoparticles (Farooq et al., 2024; Hsu et al., 2024), thin films (Aghaee et al., 2019; Hajjaji et al., 2015; Hu et al., 2017), and other nanostructures (Reghunath et al., 2021) to control these factors. Among these, spin coating method is widely adopted method for growing oxide films (Nandy and Chae, 2023; Panwar et al., 2023). It's cost-effective, time saving and easy to use method compared to physical deposition method (Yin, 2023). Thus, extensively used by researchers to grow TiO₂ films (Lukong et al., 2022; Khamkhash et al., 2022). Hence, this work is aimed to grow F doped TiO₂ films and investigate the impact of film thickness on various characteristics.

2. Experimental Details

2.1 Film Deposition

Titanium tetra Isopropoxide (TTIP), and tri fluoro acetic acid as a source of Ti and F respectively and 2-methoxy ethanol, were purchased from Sigma-Aldrich. The water utilized during the experiment was DI. No additional purification was done in the chemicals; all of the compounds were analytical grade when they were applied. Chemically and thermally stable films of TiO₂ were prepared using spin coating technique. Glass substrates were used for film deposition. The glass slides were cleaned properly. The very first step of cleaning was detergent cleaning then an ultrasonic bath with water was done, and finally, the films were dried properly. The precursor solution was prepared by using 2 methoxy ethanol as a solvent, and TTIP was used as a precursor, the solution was doped with Tri fluoro acetic acid 6%. The solution obtained was stirred at room temperature in an open atmosphere for one h. After stirring the solution was kept for 24 h for ageing. After aging the films were prepared. The solution was dispensed on the substrates from a distance of ~ 10 mm distance and a spinner was employed to spin the substrates at a speed of 2500 rpm. The film so obtained was dried at a temperature of 200°C for 10 min. After repeating this process for respective number of coatings, the films were placed for in furnace for annealing at 450°C for 1 h. Firstly, the experiment was done to optimize the thickness of the films, so the samples were prepared with various thicknesses by varying the number of coating cycles i.e. 5, 10, 15, 20, 25, 30.

2.2 Characterizations

The thickness of deposited films was estimated using Stylus profilometer. The structural properties were analyzed by using an X-ray diffraction (XRD) which operates at an accelerating voltage of 40 kV. using CuK $_{\alpha}$ radiations ($\lambda=0.15406$ nm), a rate of 6°/min. The morphologic of these TiO $_{2}$ films were achieved with a high-resolution TESCAN Model: Magna LMU scanning electron microscope (SEM) operating at an acceleration voltage of 10 kV. The film thicknesses of films were measured with a Dektak- 8-stylus profiler (stylus diamond tip radius = 12.5 mm, vertical range from 5 nm to 1 mm, stylus tracking force range from 0.03 to 15 mg). The transmittance of films was recorded by UV-VIS-NIR Spectrophotometer (Shimadzu 3600, Japan) in the range of 200 - 800 nm.

3. Results and Discussion

3.1 Thickness Analysis

The thickness of deposited F-doped TiO₂ films is 0.4, 1.0 1.6, 2.1, 2.6 and 3.2 μm for coating cycles of 5, 10, 15, 20, 25 and 30 respectively. Increase of material on the substrate with increasing coating cycle is responsible for the increase of film thickness. This is in agreement with the film grown by other methods. To get deeper insights of this effect, variation of film thickness with increase of coating cycle is shown in **Figure 1**. Variation of thickness (t) with coating cycle (n) exhibit a linear variation, which can be described by the following equation,

$$t = (0.11 \pm 0.01)n + (-0.15 \pm 0.03).$$

In case of spin coating method, similar variation of thickness with cycle number is also observed by other kind of films such as AlN (Eom et al., 2006), TiO₂ (Chen et al., 2016), ZnO (Smirnov et al., 2010), ferrite films (Yusuf and Mustaffa, 2019) etc. Such variation of film thickness in spin-coating method is explained on the basis of hydrodynamic analysis (Park, 2022).

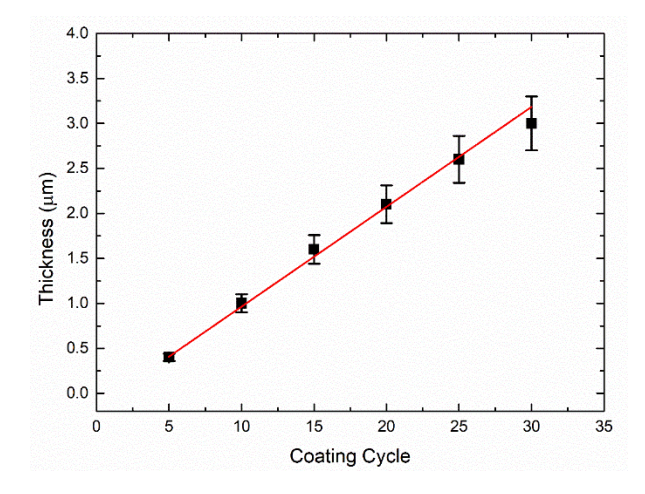


Figure 1. Variation of film thickness with coating cycle. Error bar is taken 10% of value.

3.2 Morphological Studies

Since, film thickness dependent morphology changes are characteristics of film deposited films (Taylor et al., 2011), hence morphology of selected films are investigated using SEM. SEM images of F-doped TiO₂ films for coating cycles of 10, 20 and 30 are shown in **Figure 2**. Significant changes are observed in the morphology of these films with increase of coating cycles (Grilli et al., 2018; Momeni and Ghayeb, 2016). The surface morphology of films grown at coating cycles of 10 and 20 is identical (Monazzam and Kisomi, 2017) and exhibit crack like structures. However, film grown for coating cycles of 30 layered film is smooth and shows crack-free morphology.

3.3 Crystalline Phase Study

The XRD results of these films at different coating cycles are shown in **Figure 3**. It is observed from Figure 3 that the coating cycles such as 5 and 10 shows no clear peaks, this may be due to presence of film on the substrate in amorphous nature (Pandey et al., 2016).

On further increasing, coating cycles, diffraction peak at 25 ± 0.02^0 appear in the XRD patterns. This peak is assigned to the (101) plane of tetragonal anatase phase of TiO₂ (JCPDS 21-1272) (Li et al. 2014). Other diffraction peaks located at $2\theta \sim 37.6\pm0.02$, 47.4 ± 0.02 , 53.7 ± 0.02 , 54.9 ± 0.02 , and $62.4\pm0.02^\circ$ can been seen in the patterns. These peaks are due to the contribution from (004), (200), (105), (211), (204) planes of this phase. This show that deposited TiO₂ thin films are polycrystalline with an anatase phase. Thus, XRD study shows a transformation from the amorphous to the crystalline thin films with coating cycles (**Figure 4**). This kind of transformation with deposition parameter is also observed for MgO thin films and explained on the basis of X-ray absorption spectroscopy (Singh et al., 2020). Change of XRD peak intensity is associated with change in degree of crystallization of these films (Bellardita et al., 2018; Singh et al., 2016) which is also confirmed from the value of peak width as shown in **Table 1** (Toroya, 2023).

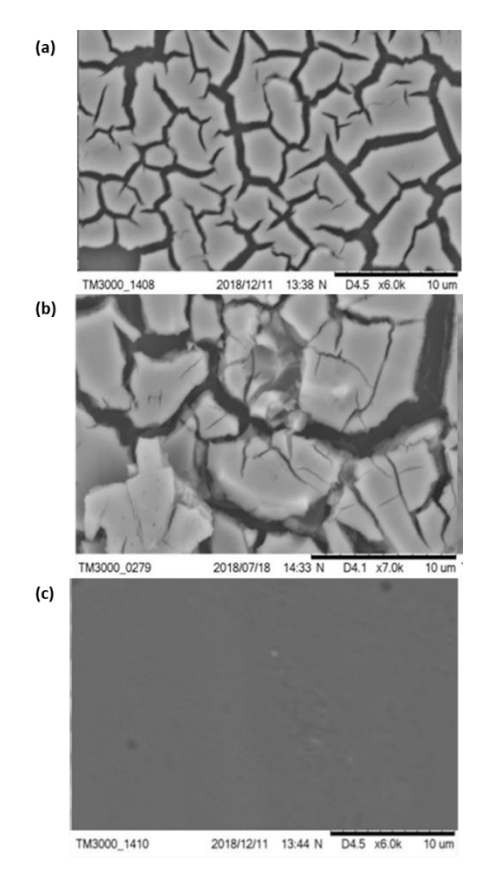


Figure 2. SEM images for (a) 10 (b) 20 (c) 30 coating cycles (Top View).

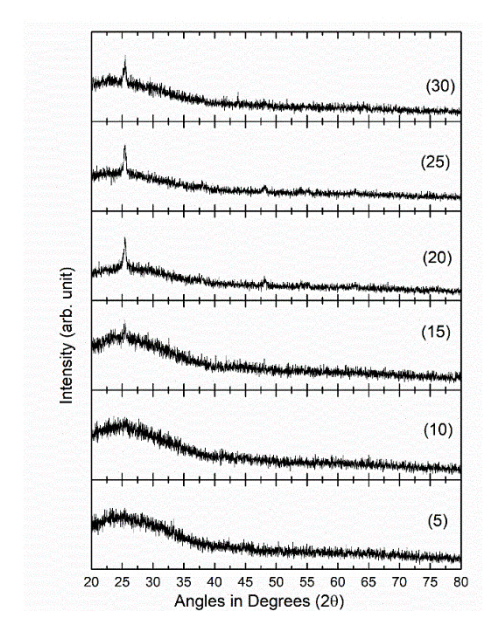


Figure 3. XRD patterns of TiO₂ thin films for different coating cycles. Values in parenthesis denotes the coating cycle number.

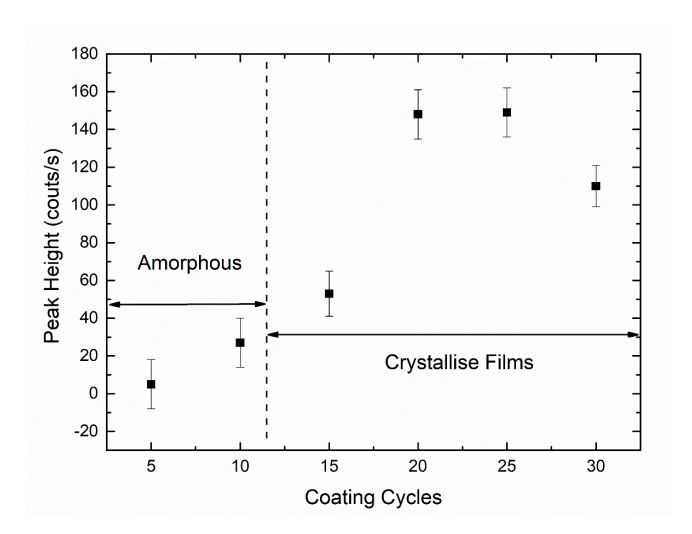


Figure 4. Schematic representation of amorphous and crystalline nature of F-doped TiO₂ films with coating cycles.

 No. of coating cycles
 Thickness (μm)
 FWHM (°)

 5
 0.4

 10
 1.0

 15
 1.6
 0.52±0.02

 20
 2.1
 0.41±0.02

 25
 2.6
 0.26±0.02

3.2

 0.15 ± 0.02

Table 1. Full-width at Half maximum (FWHM) of peak corresponding to (101) plane.

3.4 Structural Parameters

30

Structural parameters for the crystalline F-doped TiO₂ films are estimated by determining the peak position and FWHM of most intense peak in the XRD pattern shown in **Figure 3**. The crystallite size (D) of the films was determined by using the Debye-Scherrer's formula (Hassanzadeh-Tabrizi, 2023; Singh et al., 2016).

$$D = \frac{0.9\lambda}{\beta\cos\theta}nm\tag{1}$$

Here, β stands for FWHM, λ for 1.5407Å, k = 0.94, and θ for diffracting angle. The values of crystallite size are 50, 105, 157 and 198 nm for coating cycles of 10, 15, 20, 25 and 30 (**Table 2**). Thickness(t) and crystallite size can give an estimation of number of crystallites in these films (Ferro et al., 2001), Number of crystallites (N) can be estimated as follows:

$$N = \frac{t}{D^3} \tag{2}$$

Table 2. Structural parameters of TiO₂ thin film for different thickness.

Thickness (μm)	Crystallite size D (nm)	No. of crystallites N×10 ¹⁶
1.6	50	15.2
2.1	105	6.5
2.6	157	2.9
3.2	198	1.2

The growth mechanism that involves dislocation is a very significant issue. A crystal's flaw known as a dislocation result from the lattice in one area of the crystal not matching the lattice in another. Linear flaws in the crystal structure are called dislocations. The number of flaws in the crystal is measured by the dislocation density (δ) is shown in Equation (3) which is defined as the dislocation line length in the unit volume (Erdogan and Kundakçı, 2019). The following formula can be used to determine the dislocation density of the deposited films.

$$\delta = \frac{1}{D^2} \tag{3}$$

The strain (µ) of the TiO₂ films calculated by following relation using the FWHM (Ovid, 2000; Rahman and Khan, 2014).

$$\mu = \frac{\beta \cos \theta}{4} \tag{4}$$

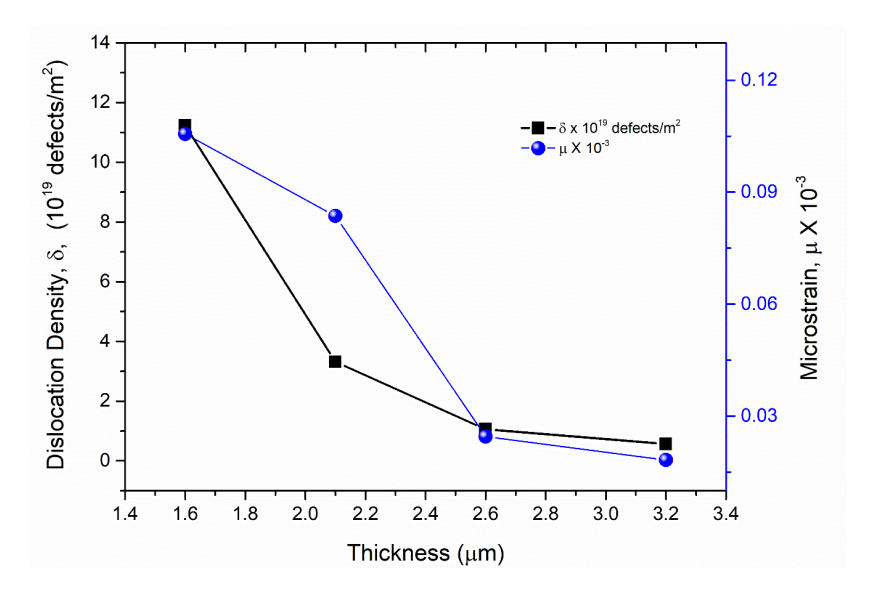


Figure 5. Variation of dislocation density and microstrain with thickness for F-doped TiO₂ films.

Figure 5 shows that both the dislocation density and micro strain decreases with increase of film thickness. Decrease of strain with thickness is due to increase in relaxation of the films at higher thicknesses (Ali et al., 2023; Qiao et al., 2004)

4. Conclusion

Using a spin coating approach, TiO₂ thin films were deposited on a glass substrate with different thickness. The film's thickness increased with increased the number of coating cycles, while the dislocation density falls. The SEM results show the films' rough surface and irregular crystalline development. Thus, this work demonstrates that coating cycles have a significant impact on the characteristics of TiO₂ thin films.

Conflict of Interest

The authors confirm that there is no conflict of interest to declare for this publication.

Acknowledgments

JKR acknowledges help and support from SRM Institute of Science and Technology, Delhi-NCR Campus, Modinagar during the course of investigation of this work.



References

- Aghaee, M., Verheyen, J., Stevens, A.A., Kessels, W.M., & Creatore, M. (2019). TiO2 thin film patterns prepared by chemical vapor deposition and atomic layer deposition using an atmospheric pressure microplasma printer. *Plasma Processes and Polymers*, 16(12), 1900127.
- Ali, B.A., Bouhmouche, A., Wendling, L., Hu, C., Bouillet, C., Schmerber, G., Saeedi A.M., Zafeiratos S., Papaefthimiou V., Moubah, R., & Colis, S. (2023). Impact of film thickness on the structural, linear and non-linear optical properties of ferroelectric Bi2FeCrO6 perovskite thin films. *Vacuum*, *216*, 112411.
- Ayorinde, T., & Sayes, C.M. (2023). An updated review of industrially relevant titanium dioxide and its environmental health effects. *Journal of Hazardous Materials Letters*, 4, 100085.
- Bellardita, M., Di Paola, A., Megna, B., & Palmisano, L. (2018). Determination of the crystallinity of TiO2 photocatalysts. *Journal of Photochemistry and Photobiology A: Chemistry*, 367, 312-320.
- Chen, W.F., Koshy, P., & Sorrell, C.C. (2016). Effects of film topology and contamination as a function of thickness on the photo-induced hydrophilicity of transparent TiO 2 thin films deposited on glass substrates by spin coating. *Journal of Materials Science*, *51*, 2465-2480.
- Choudhury, B., & Choudhury, A. (2013). Local structure modification and phase transformation of TiO 2 nanoparticles initiated by oxygen defects, grain size, and annealing temperature. *International Nano Letters*, *3*, 1-9.
- David, M., Doganlar, I.C., Nazzari, D., Arigliani, E., Wacht, D., Sistani, M., & Hinkov, B. (2024). Surface protection and activation of mid-IR plasmonic waveguides for spectroscopy of liquids. *Journal of Lightwave Technology*, 42(2), 748-759.
- De, M., Punjabi, N., Prakash, N., & Mukherji, S. (2024). Optical Fiber Based Gold Nanoparticles and Titanium Dioxide Modified in Situ Refractometer and Immunosensor. *IEEE Sensors Journal*, 24(5), 6264-6271.
- Dubey, R.S., Jadkar, S.R., & Bhorde, A.B. (2021). Synthesis and characterization of various doped TiO2 nanocrystals for dye-sensitized solar cells. *ACS Omega*, *6*(5), 3470-3482.
- Eftekhari, A., Babu, V.J., & Ramakrishna, S. (2017). Photoelectrode nanomaterials for photoelectrochemical water splitting. *International Journal of Hydrogen Energy*, 42(16), 11078-11109.
- Eom, D., No, S.Y., Hwang, C.S., & Kim, H.J. (2006). Properties of aluminum nitride thin films deposited by an alternate injection of trimethylaluminum and ammonia under ultraviolet radiation. *Journal of The Electrochemical Society*, 153(4), C229.
- Erdoğan, E., & Kundakçı, M. (2019). Investigation of GaN/InGaN thin film growth on ITO substrate by thermionic vacuum arc (TVA). *SN Applied Sciences*, *1*(1), 9. https://doi.org/10.1007/s42452-018-0013-z.
- Farooq, N., Kallem, P., ur Rehman, Z., Khan, M.I., Gupta, R.K., Tahseen, T., Mushtaq, Z., Ejaz, N., & Shanableh, A. (2024). Recent trends of titania (TiO2) based materials: A review on synthetic approaches and potential applications. *Journal of King Saud University-Science*, *36*, 103210.
- Ferro, R., Rodríguez, J.A., Vigil, O., & Morales-Acevedo, A. (2001). Chemical composition and electrical conduction mechanism for CdO: F thin films deposited by spray pyrolysis. *Materials Science and Engineering: B*, 87(1), 83-86.
- Fujishima, A., Rao, T.N., & Tryk, D.A. (2000). Titanium dioxide photocatalysis. *Journal of Photochemistry and Photobiology C: Photochemistry Reviews*, 1(1), 1-21.
- Grilli, M.L., Yilmaz, M., Aydogan, S., & Cirak, B.B. (2018). Room temperature deposition of XRD-amorphous TiO2 thin films: Investigation of device performance as a function of temperature. *Ceramics International*, 44(10), 11582-11590.
- Hajjaji, A., Amlouk, M., Gaidi, M., Bessais, B., & El Khakani, M.A. (2014). *Chromium doped TiO2 sputtered thin films: synthesis, physical investigations and applications*. Springer. ISBN: 3319133535.



- Hassanzadeh-Tabrizi, S.A. (2023). Precise calculation of crystallite size of nanomaterials: A review. *Journal of Alloys and Compounds*, 168, 171914.
- Hsu, C.Y., Mahmoud, Z.H., Abdullaev, S., Ali, F.K., Naeem, Y.A., Mizher, R.M., & Habibzadeh, S. (2024). Nano titanium oxide (nano-TiO2): a review of synthesis methods, properties, and applications. *Case Studies in Chemical and Environmental Engineering*, *9*, 100626.
- Hu, Q., Huang, J., Li, Q., Wang, C., Li, G., Chen, J., & Cao, Y. (2017). Anatase TiO₂ film composed of nanorods with predominant {110} active facets as an excellent photocatalyst for water splitting. *International Journal of Hydrogen Energy*, 42(8), 5478-5484.
- Khamkhash, L., Em, S., Molkenova, A., Hwang, Y.H., & Atabaev, T.S. (2022). Crack-free and thickness-controllable deposition of tio2–rgo thin films for solar harnessing devices. *Coatings*, *12*(2), 218.
- Lukong, V.T., Ukoba, K., & Jen, T.C. (2022). Review of self-cleaning TiO2 thin films deposited with spin coating. *The International Journal of Advanced Manufacturing Technology*, 122(9), 3525-3546.
- Marcelis, E.J., ten Elshof, J.E., & Morales-Masis, M. (2024). Titanium dioxide: a versatile earth-abundant optical material for photovoltaics. *Advanced Optical Materials*, 12, 2401423.
- Momeni, M.M., & Ghayeb, Y. (2016). Preparation of cobalt coated TiO₂ and WO₃–TiO₂ nanotube films via photo-assisted deposition with enhanced photocatalytic activity under visible light illumination. *Ceramics International*, 42(6), 7014-7022.
- Monazzam, P., & Kisomi, B.F. (2017). Co/TiO₂ nanoparticles: preparation, characterization and its application for photocatalytic degradation of methylene blue. *Desalination and Water Treatment*, 63(2017), 283-292.
- Nandy, S., & Chae, K.H. (2023). Chemical synthesis of ferrite thin films. In Singh, J.P., Chae, K.H. (eds) Ferrite Nanostructured Magnetic Materials (pp. 309-334). Woodhead Publishing. https://doi.org/10.1016/B978-0-12-823717-5.00021-8.
- Ovid ko, I.A. (2000). Interfaces and misfit defects in nanostructured and polycrystalline films. *Reviews on Advanced Materials Science*, 1, 61-107.
- Pandey, A., Dutta, S., Prakash, R., Dalal, S., Raman, R., Kapoor, A.K., & Kaur, D. (2016). Growth and evolution of residual stress of AlN films on silicon (100) wafer. *Materials Science in Semiconductor Processing*, 52, 16-23.
- Panwar, S., Kumar, V., & Purohit, L.P. (2023). Oxide thin films grown using spin-coating methods. In Kumar, P., Singh, J.P., & Kumar, V. (eds) *Defect-Induced Magnetism in Oxide Semiconductors* (pp. 109-134). Woodhead Publishing. https://doi.org/10.1016/B978-0-323-90907-5.00012-9.
- Park, H. (2022). Hydrodynamic analysis of the thickness variation in a solid film formed by a spin coating process. *Coatings*, 12(5), 698.
- Qiao, Z., Latz, R., & Mergel, D. (2004). Thickness dependence of In2O3: Sn film growth. *Thin Solid Films*, 466(1-2), 250-258.
- Rahman, M.A., & Khan, M.K.R. (2014). Effect of annealing temperature on structural, electrical and optical properties of spray pyrolytic nanocrystalline CdO thin films. *Materials Science in Semiconductor Processing*, 24, 26-33.
- Reghunath S., Pinheiro, D. Devi K.R.S (2021) A review of hierarchical nanostructures of TiO₂: advances and applications. *Applied Surface Science Advances*, *3*, 100063.
- Singh, J.P., Kim, S.H., Won, S.O., Lim, W.C., Lee, I.J., & Chae, K.H. (2016). Covalency, hybridization and valence state effects in nano-and micro-sized ZnFe 2 O 4. *CrystEngComm*, 18(15), 2701-2711.
- Singh, J.P., Kumar, M., Lim, W.C., Lee, H.H., Lee, Y.M., Lee, S., & Chae, K.H. (2020). MgO thin film growth on Si (001) by radio-frequency sputtering method. *Journal of Nanoscience and Nanotechnology*, 20(12), 7530-7534.
- Smirnov, M., Baban, C., & Rusu, G.I. (2010). Structural and optical characteristics of spin-coated ZnO thin films. *Applied Surface Science*, 256(8), 2405-2408.



- Subalakshmi, K., & Senthilselvan, J. (2018). Effect of fluorine-doped TiO2 photoanode on electron transport, recombination dynamics and improved DSSC efficiency. *Solar Energy*, *171*, 914-928.
- Taylor, A.A., Edlmayr, V., Cordill, M.J., & Dehm, G. (2011). The effect of film thickness variations in periodic cracking: Analysis and experiments. *Surface and Coatings Technology*, 206(7), 1830-1836.
- Todorova, N., Giannakopoulou, T., Vaimakis, T., & Trapalis, C. (2008). Structure tailoring of fluorine-doped TiO2 nanostructured powders. *Materials Science and Engineering: B*, 152(1-3), 50-54.
- Toraya, H. (2023). Verification of a method for determining the degree of crystallinity using experimental and computer-generated powder diffraction patterns. *Journal of Applied Crystallography*, 56(6), 1751-1763.
- Yin, Y. (2023). Advances and perspectives of spin coating techniques. *Applied and Computational Engineering*, 7, 291-301.
- Yusuf, Y., & Mustaffa, M.S. (2018). Spin-coating technique for fabricating nickel zinc nanoferrite (Ni0. 3Zn0. 7Fe2O4) thin films. In Perez-Taborda, J.A., Bernal, A.G.A. (eds) *Coatings and Thin-Film Technologies*. IntechOpen. https://doi.org/10.5772/intechopen.74351.
- Zhao, J., Wang, H., Cai, Y., Zhao, J., Gao, Z., & Song, Y.Y. (2024). The challenges and opportunities for TiO₂ nanostructures in gas sensing. *ACS Sensors*, 9(4), 1644-1655.



The original content of this work is copyright © Ram Arti Publishers. Uses under the Creative Commons Attribution 4.0 International (CC BY 4.0) license at https://creativecommons.org/licenses/by/4.0/

Publisher's Note- Ram Arti Publishers remains neutral regarding jurisdictional claims in published maps and institutional affiliations.